Super-Twisting Double Integral Sliding Mode Control For a Grid-Connected Three-Phase Inverter

Abu Sufyan and Mohsin Jamil
Department of Electrical and Computer Engineering
Faculty of Engineering and Applied Science
Memorial University of Newfoundland, St. John's, NL, A1B3X5
asufyan@mun.ca, mjamil@mun.ca

Abstract— **Grid-connected inverters (GCI) play a crucial role in injecting DC power from renewable resources into the utility grid; moreover, the current quality largely depends on the effectiveness of the adopted control strategy. This paper proposed a novel super-twisting double integral sliding mode control (SMC) algorithm for a three-phase grid-connected inverter with an LCL filter. In this study, the control algorithm is first derived based on the system's dynamic mathematical model. Then, extensive simulation studies are carried out in MATLAB and Simulink software to validate its performance. Furthermore, the controller effectiveness is rigorously assessed under challenging conditions, including a 400% grid impedance variation, a 66% system parametric variation, grid frequency variation, and higher-order grid harmonic components. Under the worst-case scenario, the total harmonic distortion (THD) value of the grid current remains under 2.6%, demonstrating the proposed controller's robustness.**

Keywords—grid-connected inverter, sliding mode, super twisting, LCL filter, nonlinear control.

I. INTRODUCTION

In recent years, renewable sources-based power generation has received great attention due to their accessibility, sustainability, and modularization. The DC power generated from these sources is often fed to the power grid by adopting voltage source inverters (VSI), which require stricter conditions to maintain the high quality of current being injected [1]. The quality of current injected into the grid is usually assessed by the total harmonics distortion (THD) level. According to the IEEE Grid Interconnection standard, the THD of the current injected into the grid must be less than 5% [2]. For reducing the higher-order harmonics components from the grid current, a single inductive filter (L) or a filter with a capacitor between two inductors (LCL) is mandatory. The LCL filter provides better harmonics reduction capability and has less inductor size compared to the L-type inverter; however, the third-order LCL filter increases control complexity and also suffers from an inherent resonance problem that arises from filter parametric variation, which can deteriorate system stability [3]. Therefore, designing an appropriate control strategy that can ensure the system's stability under extreme conditions is crucial.

Various control techniques have been proposed in the literature to inject smooth and sinusoidal current into the grid while maintaining stability. To mitigate the resonance effects, two major damping approaches have been used with current controllers, namely passive damping [4] and active damping [5]. In passive damping, oscillations are dampened by simply adding a passive component like a resistor, capacitor, or inductor. In [4], [6], and [7], applied the passive damping approach to control the grid-connected inverter, the results are satisfactory under certain conditions; however, the use of extra passive components leads to excessive power loss in larger

systems. To avoid power losses, an active damping approach has been implemented in [5], [8]–[10] that utilizes a feed-forward or feedback-damping signal in the control loop for stabilizing the system. Nevertheless, these control loops cannot entirely eliminate the control delay that exists in digital controllers, which compromises the controller reference tracking performance. Furthermore, these strategies are implemented using proportional and proportional integral control, which has poor AC signal-tracking performance; therefore, it requires transformation into the synchronous frame of reference, and even in the synchronous frame, controller performance degrades under grid harmonics [11]. Another controller that is commonly found in GCI literature is proportional resonant, which got special attention because of its effectiveness in tracking sinusoidal signals [11], [12]. Nevertheless, the PR controller lacks the ability to maintain GCI system stability under grid harmonics and system parametric variation.

In recent years, sliding mode control (SMC), a nonlinear control algorithm, has gained importance due to its attractive features, such as robustness, fast dynamic response, and easy implementation. However, the classical SMC suffers from the chattering problem, which introduces high-frequency oscillations in the control signal. In addition, the error variables lack convergence to origin in a finite period, leading to poor reference tracking. Due to these facts, in most literature, the SMC has been applied with a combination of proportional and proportional resonant controllers [13], [14],[15],[16]. In [13], SMC is applied on the converter side of the GCI system, and PR is the main controller to regulate the grid current, while in [14],[15], and [16] PR controller is applied to generate the capacitor voltage reference while SMC regulates the grid current. These strategies can work well under normal conditions; however, under grid impedance variation, the PR control exhibits a slow transient response, which can degrade the entire control performance and may lead to instability.

To take benefit of the useful features of SMC entirely by countering the chattering problems, the classical SMC has been extended as integral SMC [17], [18], linearized SMC [19], and super-twisting SMC [20]. Z. Li *et al.* [17] implemented integral SMC to regulate the grid current; however, this application does not involve an LCL filter for which performance may differ. In [18], integral action is added to the SMC sliding surface to reduce steady-state error. The analysis in this study is only limited to grid distortions and load variation, while grid impedance and frequency variations are not considered. A linearized SMC is proposed in [19], to inject current into utility grid under filter parametric variation. However, it involves complex procedures to construct transfer function and exhaustive analysis for closed loop pole selections. In [20], a super-twisting control is implemented for

a three-phase GCI system under grid impedance variation and grid harmonics. However, this study lacks the analysis of controller performance under grid frequency variation and 66% filter parametric variation from nominal value.

This research proposes a novel robust super-twisting double integral sliding mode control for GCI with an LCL filter under external disturbances. The main contributions of this work are listed below:

- Super-twisting double integral SMC control design in stationary reference frame to reduce synchronous frame transformation computation.

- Stability of entire GCI system under variation of frequency, inductance, grid voltage and filter parameter.

- Detailed mathematical design of controller.

II. SYSTEM MATHEMATICAL MODELING

Fig.1 depicts the composition of a three-phase grid-connected VSI with an LCL filter. The LCL filter contains an inductor L_1 and a resistor r_1 on the inverter side, an inductor L_2 and resistor r_2 on the grid side, and a filter capacitor C between them. The two-level VSI comprises three legs, with two switching devices on each of the legs, that are controlled by the PWM signals generated by the controller. From the input DC side, VSI is connected to a stable DC voltage source V_{dc}, and the output AC side is connected to the grid V_g. The GCI system state-space mathematical model is can be given from the circuit as follows:

$$L_1 \frac{di_{1k}}{dt} = v_{ik} - i_{1k}r_1 - v_{ck} \tag{1}$$

$$L_2 \frac{di_2 k}{dt} = v_{ck} - i_2 r_2 - v_{gk} \tag{2}$$

$$C \frac{dv_{ck}}{dt} = i_{1k} - i_{2k} \tag{3}$$

Where $k = (a, b, c)$ represents three-phases of GCI system, v_{ik}, i_{2k}, i_{1k}, v_{ck} and v_{gk} represent the inverter output voltage, grid current, capacitor voltage, and grid voltage respectively. Generally, grid current under ideal conditions is expected to appear in phase with grid voltages. Considering the grid voltage, a sinusoidal signal that can be given as v_{gk} $Cos(wt + \theta)$, then the grid current reference can be taken in the form of

$$i_{2k}^* = I_2 \sin(\omega t + \theta) \tag{4}$$

Where I_2 is the amplitude of i_{2k} and θ is the phase angle of grid voltages

III. ERROR MODEL DESIGN

In order to design a controller, an appropriate error model consisting of the reference values is required. The error signal includes the reference signal we want to track and actual system signal. Here, in order to achieve best tracking performance error signal for grid current, inverter current, capacitor voltage and double integral of grid current is taken as given below:
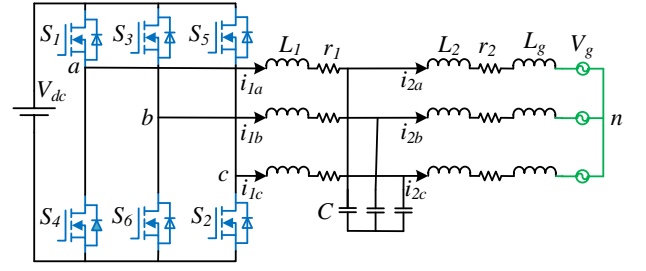

Fig. 1. GCI voltage source inverter with an LCL filter

$$e_1 = i_1^* - i_1 \tag{5}$$

$$e_2 = v_c^* - v_c \tag{6}$$

$$e_3 = i_2^* - i_2 \tag{7}$$

$$e_4 = \int (i_2^* - i_2)\, dt \tag{8}$$

$$e_5 = \int \left[\int (i_2^* - i_2)\, dt \right] dt \tag{9}$$

Now to drive error dynamical model take the time derivative of eq. (5) – (9) and simplifying them yields the following:

$$\dot{e}_1 = -\frac{r_1}{L_1} e_1 - \frac{1}{L_1} e_2 + \frac{1}{L_1} v_c^* - \frac{1}{L_1} v_i + \dot{i}_1^* + \frac{r_1}{L_1} i_1^* \tag{10}$$

$$\dot{e}_2 = \frac{1}{C} e_1 - \frac{1}{C} e_3 \tag{11}$$

$$\dot{e}_2 = \frac{1}{L_2} e_2 - \frac{r_2}{L_2} e_3 \tag{12}$$

$$\dot{e}_4 = e_3 \tag{13}$$

$$\dot{e}_5 = e_4 \tag{14}$$

IV. CONTROLLER DESIGN

The sliding surface design plays a crucial role in the system dynamics of finite-time convergence. In conventional SMC, the sliding surface is combination of linear state variables; although its design is simple and easy to implement, however, the convergence of states is slower and steady state error degrade reference tracking performance. Therefore, in the design of double integral SMC, double integral term is added in error model to eliminate the reference tracking error entirely.

$$S = \alpha_1 e_1 + \alpha_2 e_2 + \alpha_3 e_3 + \alpha_4 e_4 + \alpha_5 e_5 \tag{15}$$

Where, α_1, α_2, α_3, α_4, α_5 are sliding surface coefficients to control the trajectories motion. Now taking the time derivative of (1) yields

$$\dot{S} = \alpha_1 \dot{e}_1 + \alpha_2 \dot{e}_2 + \alpha_3 \dot{e}_3 + \alpha_4 \dot{e}_4 + \alpha_5 \dot{e}_5 \tag{16}$$

Putting error dynamics from (10) – (15) into (16) gives:

$$\dot{S} = \alpha_1 \left(\dot{i}_1^* - \frac{r_1}{L_1} e_1 - \frac{1}{L_1} e_2 + \frac{r_1}{L_1} i_1^* + \frac{1}{L_1} v_c^* - \frac{1}{L_1} v_i \right) +$$

$$\alpha_2 \left(\frac{1}{C} e_1 - \frac{1}{C} e_3 \right) + \alpha_3 \left(\frac{1}{L_2} e_2 - \frac{r_2}{L_2} e_3 \right)$$

$$+ \alpha_4 e_3 + \alpha_5 e_4 \qquad (17)$$

To ensure that the system trajectories enter the sliding surface manifold in finite time, a reaching law is combined with the main control to boost the trajectories convergence rate [21], which is given as follows

$$\dot{S} = -\gamma \, |S|^{\varsigma} \, sign(S) \qquad (18)$$

Where $\gamma>0$ is design parameter and ζ is a constant in the range of $0 < \zeta <1$ which decide the rate of convergence of system states to sliding surface. Once the trajectories enter the sliding surface, they gradually reach to equilibrium state which results in S=0, that leads to

$$\dot{S} = 0 \qquad (19)$$

Now to find the equivalent SMC law compare (17) and (19) which gives:

$$u_{eq} = L_1 \dot{i}_1^* - r_1 e_1 - e_2 + r_1 i_1^* + v_c^* + \frac{L_1}{C} \frac{\alpha_2}{\alpha_1} e_1 + \frac{L_1}{L_2} \frac{\alpha_3}{\alpha_1} e_2$$

$$- \frac{L_1}{C} \frac{\alpha_2}{\alpha_1} e_3 - \frac{L_1}{L_2} \frac{\alpha_3}{\alpha_1} r_2 e_3 + \frac{L_1 \alpha_4}{\alpha_1} e_3 + \frac{L_1 \alpha_5}{\alpha_1} e_4 \quad (20)$$

Now the switching control can be obtained from (18) as follows:

$$u_{sw} = -\gamma \, |S|^{\varsigma} \, sign(S), \quad \gamma > 0 \qquad (21)$$

So, the final double integral SMC law can be written as follows.

$$u_{SMC} = u_{eq} + u_{sw} \qquad (22)$$

Next, super-twisting control (STC) is implemented which yields continuous control signal that comprehensively reduces the chattering problems with SMC. The STC consists of two terms, that of a continuous time function and integral of sliding surface function which is given as:

$$u_{STC}(t) = \begin{cases} -Z_1 \sqrt{|S|} sign(S) + u_1 \\ \dot{u}_1 = -Z_2 sign(S) \end{cases} \qquad (23)$$

Where, Z_1, and Z_2 are control gains. The controller in (23) can be written in compact form as

$$u_{STC} = -Z_1 \sqrt{|S|} sign(S) - Z_2 \int sign(S) d(\tau) \quad (24)$$

Finally, the global super-twisting double integral sliding mode control (ST-DISMC) law can be obtained by putting (22) and (24) as

$$u_{ST-DISMC} = u_{STC} + u_{SMC} \qquad (25)$$

Now to verify the stability of control in (25), Lyapunov stability analysis is carried out. For, this a Lyapunov function is taken which is given as:

$$V = \frac{1}{2} S^2 \qquad (26)$$

Taking time derivative of (26) and putting (17) in it yields:

$$\dot{V} = S \left(\alpha_1 \left(\dot{i}_1^* - \frac{r_1}{L_1} e_1 - \frac{1}{L_1} e_2 + \frac{r_1}{L_1} i_1^* + \frac{1}{L_1} v_c^* - \frac{1}{L_1} v_i \right) + \right.$$

$$\left. \alpha_2 \left(\frac{1}{C} e_1 - \frac{1}{C} e_3 \right) + \alpha_4 e_3 + \alpha_5 e_4 + \alpha_3 \left(\frac{1}{L_2} e_2 - \frac{r_2}{L_2} e_3 \right) \right)$$

$$(27)$$

Now, putting control law from (15) in (27) gives

$$\dot{V} = S \left(-\gamma \, |S|^{\varsigma} \, sign(S) - Z_1 \sqrt{|S|} sign(S) \right.$$

$$\left. - Z_2 \int sign(S) d(\tau) \right) \qquad (28)$$

$$\dot{V} = -\gamma \, |S| |S|^{\varsigma} \, sign(S) - Z_1 |S| \sqrt{|S|} sign(S)$$

$$- Z_2 |S| \int sign(S) d(\tau) \right) \qquad (29)$$

$$\dot{V} < 0, \ \forall \ \gamma > 0 \qquad (30)$$

So, the Lyapunov function results negative definite which means the ST-DISMC control law is globally asymptotically stable, and systems states will converge to sliding surface in finite time.

TABLE I.   SYSTEM PARAMETERS

Parameters	Symbol	Value
DC input voltage	V_{dc}	350V
Filter Inductors	L_1, L_2	1.3 mH
Capacitance	C	6.5 μF
Filter Inductor resistance	r_1, r_2	0.22 Ω
Grid supply voltage	V_g	110 V
Switching frequency	F_{sw}	14 KHz
Sliding coefficients	$\alpha_1, \alpha_2, \alpha_3, \alpha_4, \alpha_5$	10, 1.5, 700, 5, 8000
Super-twisting coefficients	Z_1, Z_2, γ	[8,15, 10] $* 10^5$
	ζ	0.9

V. SIMULATION RESULTS

To analyze the performance of the proposed controller, the mathematical design of controller is implemented in MATLAB and Simulink software environments, for which the controller parameters are illustrated in Table 1. First, to test the controller performance under steady state the waveform for current injected into the utility grid is depicted in Fig. 2(a). The results shows that the THD of the grid current waveform in nominal conditions is 1.4% which

exhibits the characteristics of a pure sinusoidal waveform. Fig. 2(b) shows the current injected into grid has same phase angle as the grid voltages, which means a unity power factor is maintained during this operation. In GCI operation under disturbance controller tracking performance can be degraded, to analyze the reference tracking performance a step change of 10A is added in current reference value at t = 0.05s. The waveforms in Fig. 2(c) show that the proposed controller tracks the reference value efficiently. In grid-connected inverters the grid frequency and voltage variation can boost the harmonics in grid current or event can lead to instability, to show the controller robustness under this condition 1.5Hz variation in grid frequency and grid voltage harmonics of 2nd to 11th is considered for which the fast Fourier transform of grid current waveform is given in Fig. 3(a) and Fig. 3(b) respectively.

These results are evident that the controller suppresses the disturbances effectively. Other issues that lead to instability in grid-connected inverters are grid inductance variation and filter parametric variation due to ageing effects. To evaluate performance under these circumstances, the value of grid inductance is varied 400% from nominal value and the filter inductance is varied 66%. The current waveforms in Fig. 4 and Fig. 5 show that the THD of grid current is 1.9% and 1.84% respectively, which is far below the IEEE requirement of 5% for grid connection.

Fig. 3. Controller performance under grid disturbances. (a) grid frequency variation from 50Hz to 48.5Hz. (b) Utility grid odd harmonics of 2nd to 11th order.
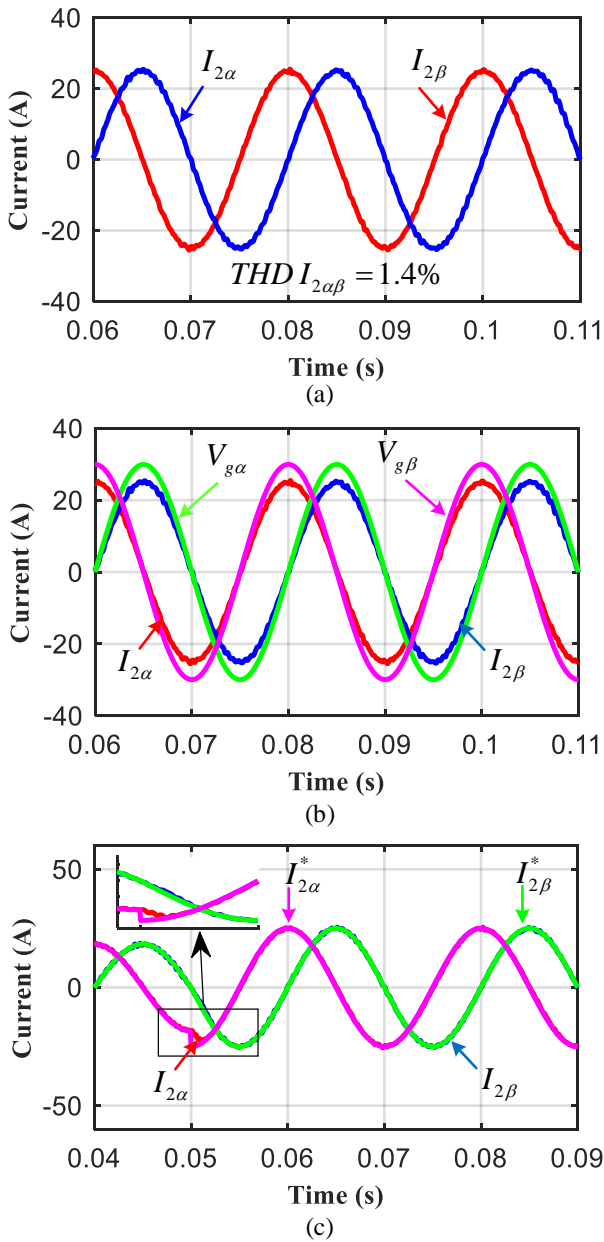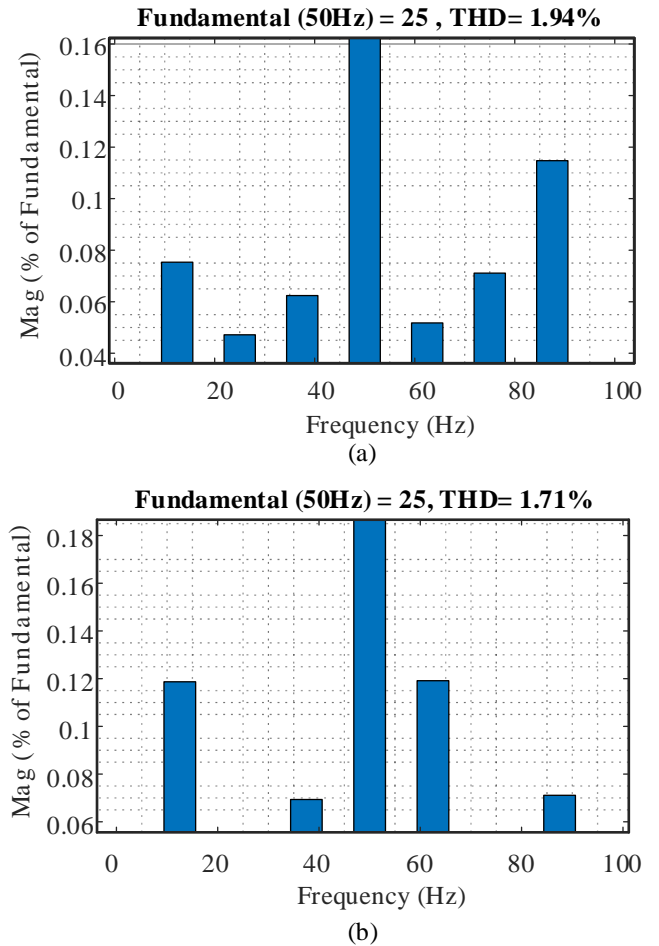

Fig. 2. ST-DISMC Controller performance in steady state: (a) current injected into grid. (b) Grid current and voltage in phase. (c) reference tracking performance during a step change of 10A.
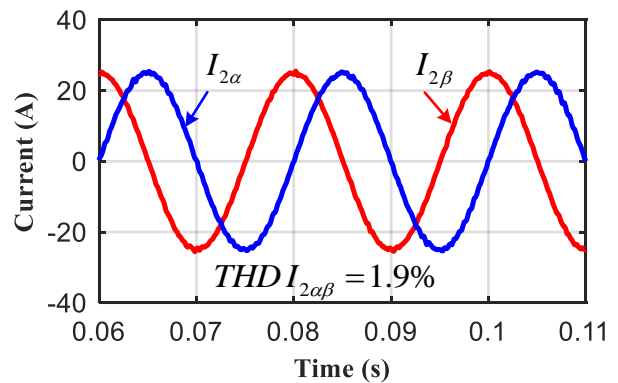

Fig. 4. ST-DISMC performance under inductance variation of 400% from nominal value.
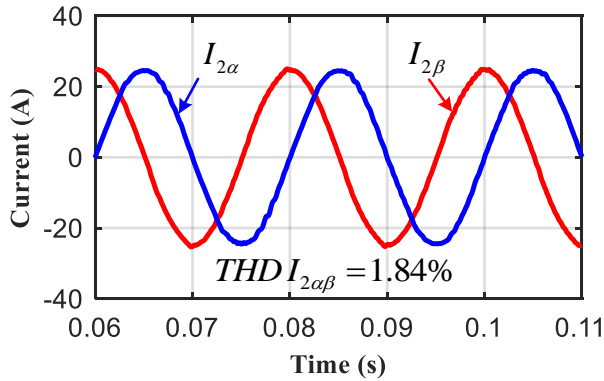
Fig. 5. ST-DISMC performance under filter parametric variation of 66%.

VI. Conclusion

This research proposes a robust Super-twisting double integral sliding mode controller for the GCI system under external disturbances. A new error model dynamical system is presented to enhance the quality of current injected into the grid current with almost zero steady-state error. The simulation results show that the controller can inject high quality current into the grid even under filter parametric variation of 66%, grid inductance variation of 400%, grid frequency variation of 1.5Hz and higher order grid harmonics.

References

[1]   Y. Xue and J. M. Guerrero, "Smart inverters for utility and industry applications," *PCIM Eur. 2015; Int. Exhib. Conf. Power Electron. Intell. Motion, Renew. Energy Energy Manag. Proc.*, no. May, pp. 19–21, 2015.

[2]   D. Photovoltaics, E. S.-I. Std, and undefined 2018, "IEEE standard for interconnection and interoperability of distributed energy resources with associated electric power systems interfaces," *ieeexplore.ieee.org*, Accessed: Oct. 17, 2023. [Online]. Available: https://ieeexplore.ieee.org/abstract/document/8332112/

[3]   X. Ruan, X. Wang, D. Pan, D. Yang, W. Li, and C. Bao, "Control Techniques for LCL-Type Grid-Connected Inverters," 2018, doi: 10.1007/978-981-10-4277-5.

[4]   R. N. Beres, X. Wang, F. Blaabjerg, M. Liserre, and C. L. Bak, "Optimal design of high-order passive-damped filters for grid-connected applications," *IEEE Trans. Power Electron.*, vol. 31, no. 3, pp. 2083–2098, 2016, doi: 10.1109/TPEL.2015.2441299.

[5]   C. Xie, K. Li, J. Zou, … D. L.-I. T. on, and U. 2020, "Passivity-based design of grid-side current-controlled $ LCL $-type grid-connected inverters," *ieeexplore.ieee.org*

[6]   J. Wang, X. Mu, and Q. K. Li, "Study of Passivity-Based Decoupling Control of T-NPC PV Grid-Connected Inverter," *IEEE Trans. Ind. Electron.*, vol. 64, no. 9, pp. 7542–7551, Sep. 2017, doi: 10.1109/TIE.2017.2677341.

[7]   T. Kato, K. Inoue, and Y. Yamamoto, "Optimal Digital Controller Design for Passive Stabilization of a Grid-Connected Three-Phase Inverter with LCL filter," *2019 IEEE Energy Convers. Congr. Expo.*

ECCE 2019, pp. 455–461, Sep. 2019, doi: 10.1109/ECCE.2019.8912644.

[8]   S. Gulur, V. M. Iyer, and S. Bhattacharya, "A Dual-Loop Current Control Structure with Improved Disturbance Rejection for Grid-Connected Converters," *IEEE Trans. Power Electron.*, vol. 34, no. 10, pp. 10233–10244, Oct. 2019, doi: 10.1109/TPEL.2019.2891686.

[9]   J. M. Gonzalez, C. A. Busada, and J. A. Solsona, "A Robust Controller for a Grid-Tied Inverter Connected Through an LCL Filter," *IEEE J. Emerg. Sel. Top. Ind. Electron.*, vol. 2, no. 1, pp. 82–89, 2020, doi: 10.1109/jestie.2020.3014834.

[10]   S. Li and H. Lin, "A Capacitor-Current-Feedback Positive Active Damping Control Strategy for LCL-Type Grid-Connected Inverter to Achieve High Robustness," *IEEE Trans. Power Electron.*, vol. 37, no. 6, pp. 6462–6474, 2022, doi: 10.1109/TPEL.2021.3137845.

[11]   R. Teodorescu, F. Blaabjerg, U. Borup, and M. Liserre, "A new control structure for grid-connected LCL PV inverters with zero steady-state error and selective harmonic compensation," *Conf. Proc. - IEEE Appl. Power Electron. Conf. Expo. - APEC*, vol. 1, no. February, pp. 580–586, 2004, doi: 10.1109/apec.2004.1295865.

[12]   T. D. C. Busarello, J. A. Pomilio, and M. G. Simoes, "Design Procedure for a Digital Proportional-Resonant Current Controller in a Grid Connected Inverter," *2018 IEEE 4th South. Power Electron. Conf. SPEC 2018*, 2019, doi: 10.1109/SPEC.2018.8636052.

[13]   R. Vieira, L. Martins, … J. M.-I. T. on, and U. 2017, "Sliding controller in a multiloop framework for a grid-connected VSI with LCL filter," *RP Vieira, LT Martins, JR Massing, M Stefanello IEEE Trans. Ind. Electron. 2017,*

[14]   X. Zheng, K. Qiu, L. Hou, Z. Liu, and C. Wang, "Sliding-mode control for grid-connected inverter with a passive damped LCL filter," in *Proceedings of the 13th IEEE Conference on Industrial Electronics and Applications, ICIEA 2018*, 2018, pp. 739–744. doi: 10.1109/ICIEA.2018.8397811.

[15]   N. Altin, S. Ozdemir, H. Komurcugil, and I. Sefa, "Sliding-Mode Control in Natural Frame with Reduced Number of Sensors for Three-Phase Grid-Tied LCL-Interfaced Inverters," *IEEE Trans. Ind. Electron.*, vol. 66, no. 4, pp. 2903–2913, 2019, doi: 10.1109/TIE.2018.2847675.

[16]   X. Hao, X. Yang, T. Liu, L. Huang, and W. Chen, "A sliding-mode controller with multiresonant sliding surface for single-phase grid-connected VSI with an LCL filter," *IEEE Trans. Power Electron.*, vol. 28, no. 5, pp. 2259–2268, 2013, doi: 10.1109/TPEL.2012.2218133.

[17]   K. Rayane, M. Bougrine, H. Abu-Rub, A. Benalia, and M. Trabelsi, "Average Model-Based Sliding Mode Control for Quality Improvement of a Grid-Connected PUC Inverter," *IEEE J. Emerg. Sel. Top. Power Electron.*, vol. 11, no. 4, pp. 3765–3774, Aug. 2023, doi: 10.1109/JESTPE.2023.3264856.

[18]   Z. Li *et al.*, "Virtual Synchronous Generator and SMC-Based Cascaded Control for Voltage-Source Grid-Supporting Inverters," *IEEE J. Emerg. Sel. Top. Power Electron.*, vol. 10, no. 3, pp. 2722–2736, 2022, doi: 10.1109/JESTPE.2021.3056576.

[19]   H. Li, W. Wu, M. Huang, H. Shu-Hung Chung, M. Liserre, and F. Blaabjerg, "Design of PWM-SMC Controller Using Linearized Model for Grid-Connected Inverter with LCL Filter," *IEEE Trans. Power Electron.*, vol. 35, no. 12, pp. 12773–12786, Dec. 2020, doi: 10.1109/TPEL.2020.2990496.

[20]   A. Sufyan *et al.*, "A Robust Nonlinear Sliding Mode Controller for a Three-Phase Grid-Connected Inverter with an LCL Filter," *Energies 2022, Vol. 15, Page 9428*, vol. 15, no. 24, p. 9428, Dec. 2022, doi: 10.3390/EN15249428.

[21]   M. B. Delghavi, S. Shoja-Majidabad, and A. Yazdani, "Fractional-Order Sliding-Mode Control of Islanded Distributed Energy Resource Systems," *IEEE Trans. Sustain. Energy*, vol. 7, no. 4, pp. 1482–1491, Oct. 2016